Supporting Information:

Understanding Summertime Peroxyacetyl Nitrate (PAN) Formation and Its Relation to Aerosol Pollution: Insights from High-Resolution Measurements and Modeling

Baoye Hu[1,3,4], Naihua Chen[1,6], Rui Li[7], Mingqiang Huang[1,3,4], Jinsheng Chen[2,5*], Youwei Hong[2,5], Lingling Xu[2,5], Xiaolong Fan[2,5], Mengren Li[2,5], Lei Tong[2], Qiuping Zheng[8], Yuxiang Yang[6]

[1]College of Chemistry, Chemical Engineering and Environment, Minnan Normal University, Zhangzhou, China, 363000

[2]Center for Excellence in Regional Atmospheric Environment, Institute of Urban Environment, Chinese Academy of Sciences, Xiamen 361021, China

[3]Fujian Provincial Key Laboratory of Modern Analytical Science and Separation Technology, Minnan Normal University, Zhangzhou, China, 363000

[4]Fujian Province University Key Laboratory of Pollution Monitoring and Control, Minnan Normal University, Zhangzhou, China, 363000

[5]Fujian Key Laboratory of Atmospheric Ozone Pollution Prevention, Chinese Academy of Sciences, Xiamen 361021, China

[6]Pingtan Environmental Monitoring Center of Fujian, Pingtan 350400, China

[7]Key Laboratory of Geographic Information Science of the Ministry of Education, School of Geographic Science, East China Normal University, Shanghai 200241, PR China

[8]Xiamen Key Laboratory of Straits Meteorology, Xiamen Meteorological Bureau, Xiamen 361012, China

Correspondence to: Jinsheng Chen (jschen@iue.ac.cn) & Yuxiang Yang (907460293@qq.com)

The index of agreement (IOA) is calculated by the eq. S1 (Ghahremanloo et al., 2021):

$$IOA = 1 - \frac{\sum_{i=1}^{n}(S_i - O_i)^2}{\sum_{i=1}^{n}(|S_i - \bar{O}| + |O_i - \bar{O}|)^2} \quad \text{(S1)}$$

Where, O_i denotes the observed values, $\bar{O}$ is the average observed values, S_i represents the simulated value, and n is the number of samples.

To compare the PAN production rates (P(PAN)) from observations and simulations, which were determined using Eq. S2 (Xu et al., 2021):

$$P(PAN) = \frac{PAN_2 - PAN_1}{t_2 - t_1} \quad \text{(S2)}$$

where t_1 and t_2 represent the start and end times, respectively, of the local photochemical PAN production identified for each day based on simulation results, and PAN_1 and PAN_2 are the corresponding PAN concentrations.

The net production of PAN ($Net(PAN)$) involved the production pathway of PA+NO_2, and the loss of PAN was thermal decomposition and PAN+OH during the daytime (5:00-18:00 local time) (Liu et al., 2022; Zeng et al., 2019). The net production of PAN was calculated from eq. S3:

$$Net(PAN) = k_{PA+NO_2}[PA][NO_2] - k_{PAN}[PAN] - k_{PAN+OH}[PAN][OH] \quad \text{(S3)}$$

The relative incremental reactivity (RIR) was calculated based on modeling results to reflect the sensitivity of PAN formation toward its precursor levels. If the RIR value was positive, it meant that the increase of precursors enhances PAN formation, whereas negative RIR value indicated that the increase of precursors inhibited PAN production. Besides, the greater the absolute value of RIR, the more sensitive PAN formation is to this precursor. The RIR value was calculated from eq. S4:

$$RIR_x = \frac{\frac{Net(PAN_x) - Net(PAN_{x-\Delta x})}{Net(PAN_x)}}{\Delta x / x} \quad \text{(S4)}$$

Where x represents a certain PAN precursor (e.g., NOx, C_5H_8, O_3, and HONO). $\Delta x/x$ represents the hypothetical change of mixing ratio of x (20% in this study). During simulations of O_3 and HONO, the model was not constrained by the OH modelling considering that O_3 and HONO contribute to PAN production through formation of OH (Xue et al., 2014) (Figure S2).

the root-mean-squared error (RMSE) and mean absolute error (MAE) are calculated using eq. S5 and eq. S6, respectively (Hodson, 2022):

$$RMSE = \sqrt{\frac{1}{n}\sum_{i=1}^{n}(y_i - \hat{y}_i)^2} \quad \text{(S5)}$$

$$MAE = \frac{1}{n}\sum_{i=1}^{n}|y_i - \hat{y}_i| \quad \text{(S6)}$$

Where n is the number of observations, y_i is the observed value, and $\hat{y}$ is the model's predicted value.

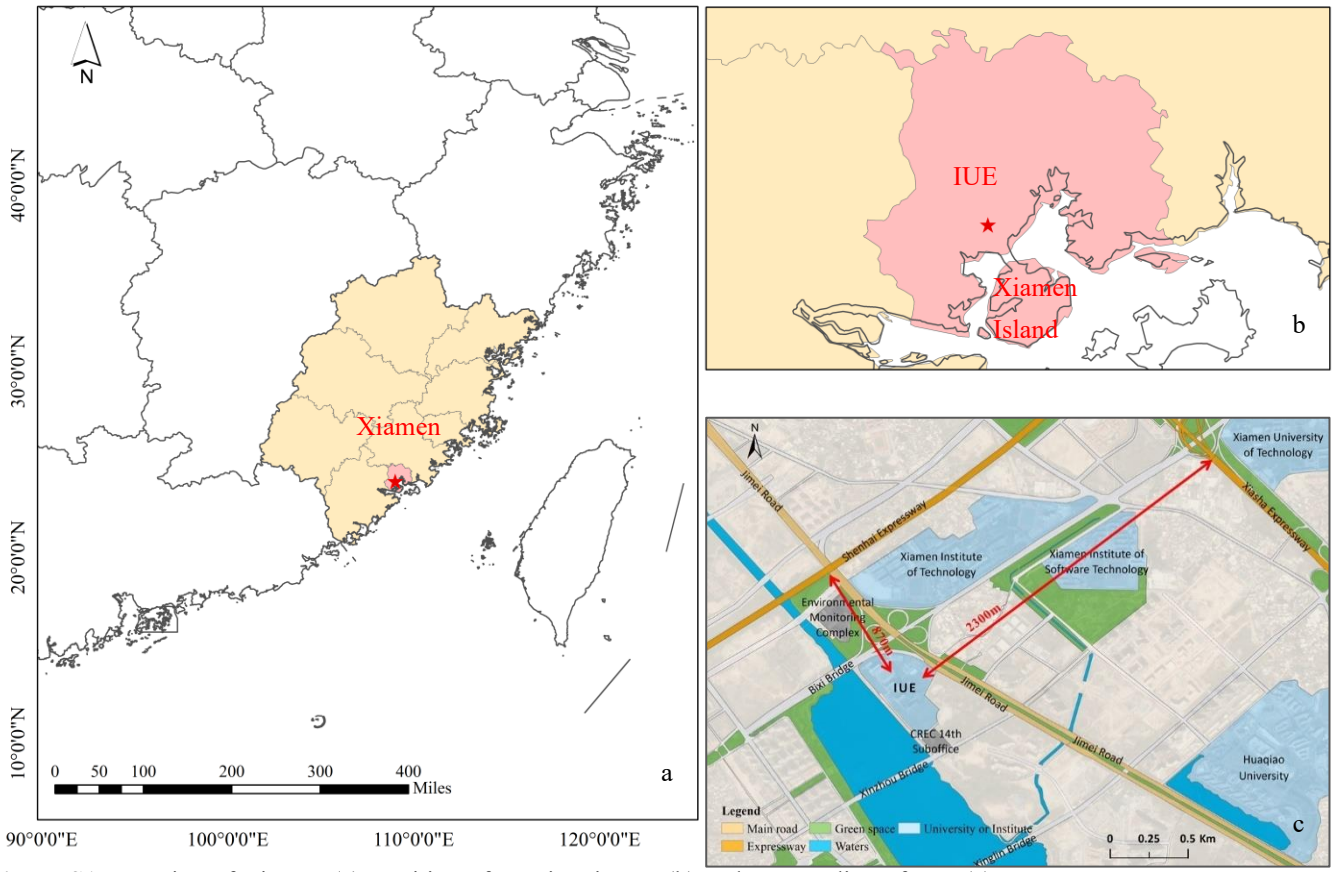

Figure S1. Location of Xiamen (a), position of IUE in Xiamen (b) and surrounding of IUE (c).

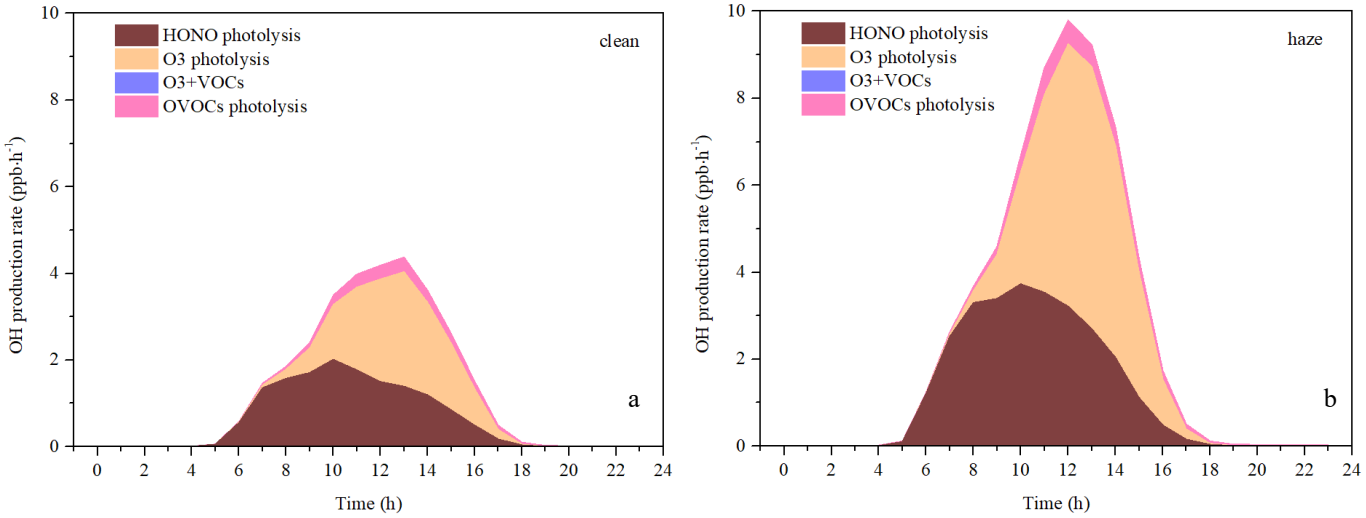

Figure S2. Model-simulated average primary production rates of OH during clean (a) and haze days (b).

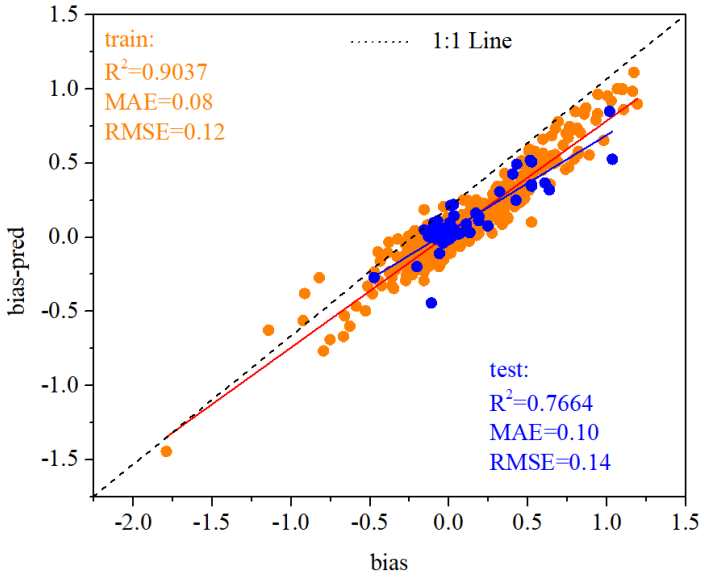

Figure S3. Model performance of XGBoost model. Orange dots represent the train set, blue dots represent the test set, and dotted black lines represent 1:1

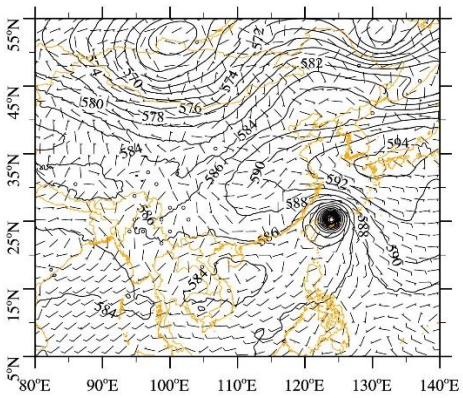

2018-7-10 12:00 UTC

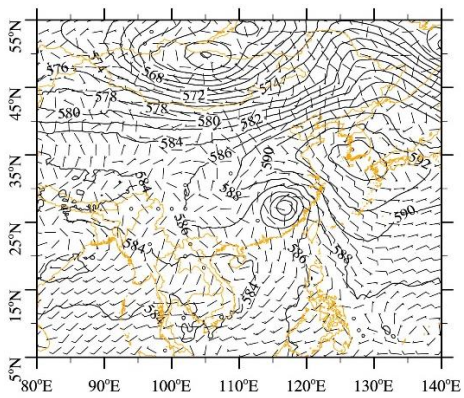

2018-7-11 12:00 UTC

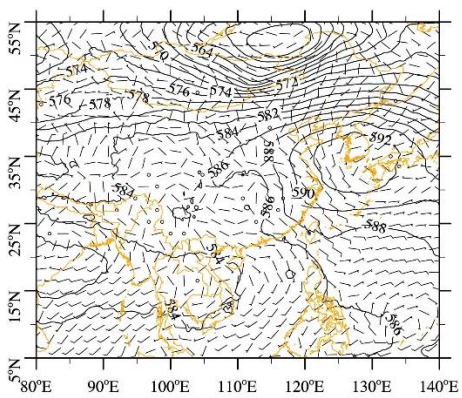

2018-7-12 12:00 UTC

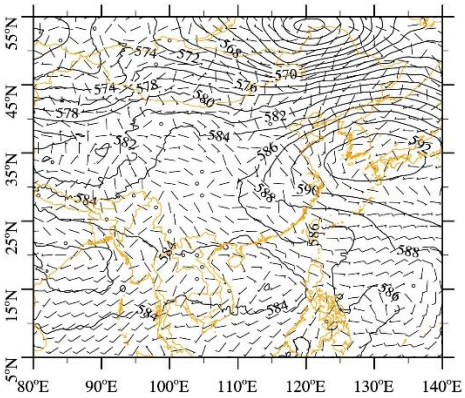

2018-7-13 12:00 UTC

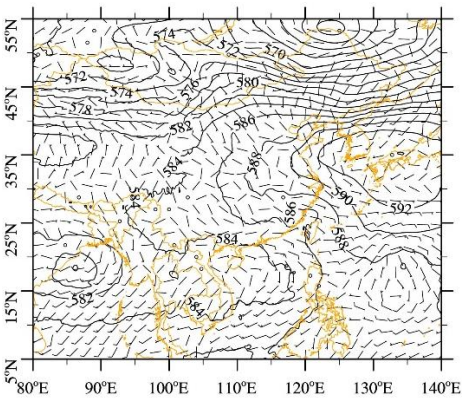

2018-7-14 12:00 UTC

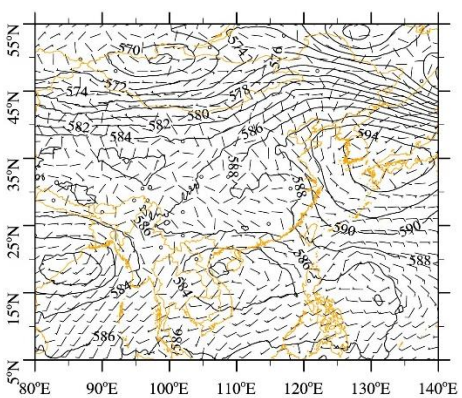

2018-7-15 12:00 UTC

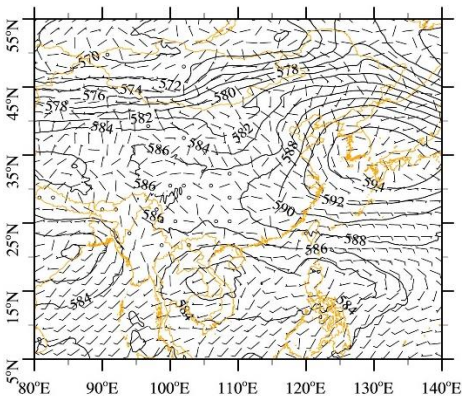

2018-7-16 12:00 UTC

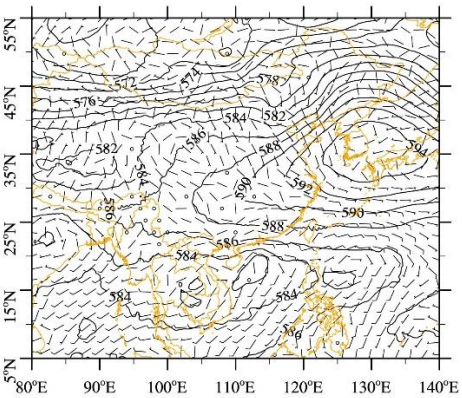

2018-7-17 12:00 UTC

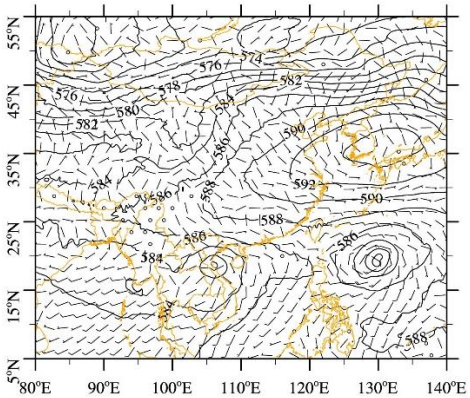

2018-7-18 12:00 UTC

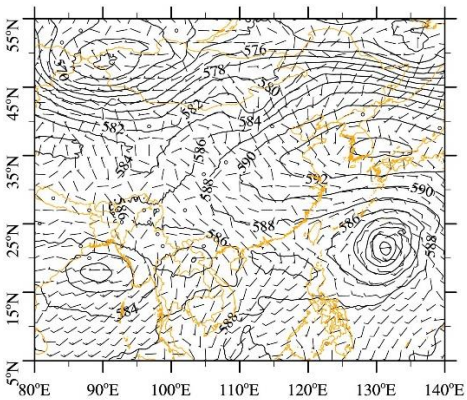

2018-7-19 12:00 UTC

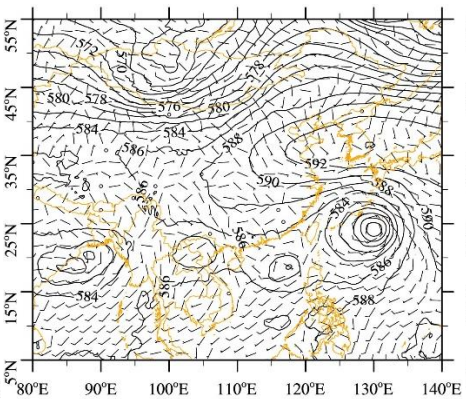

2018-7-20 12:00 UTC

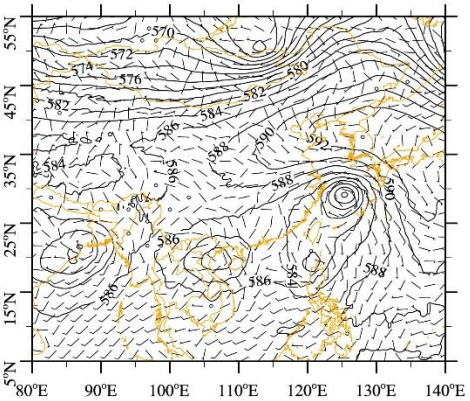

2018-7-21 12:00 UTC

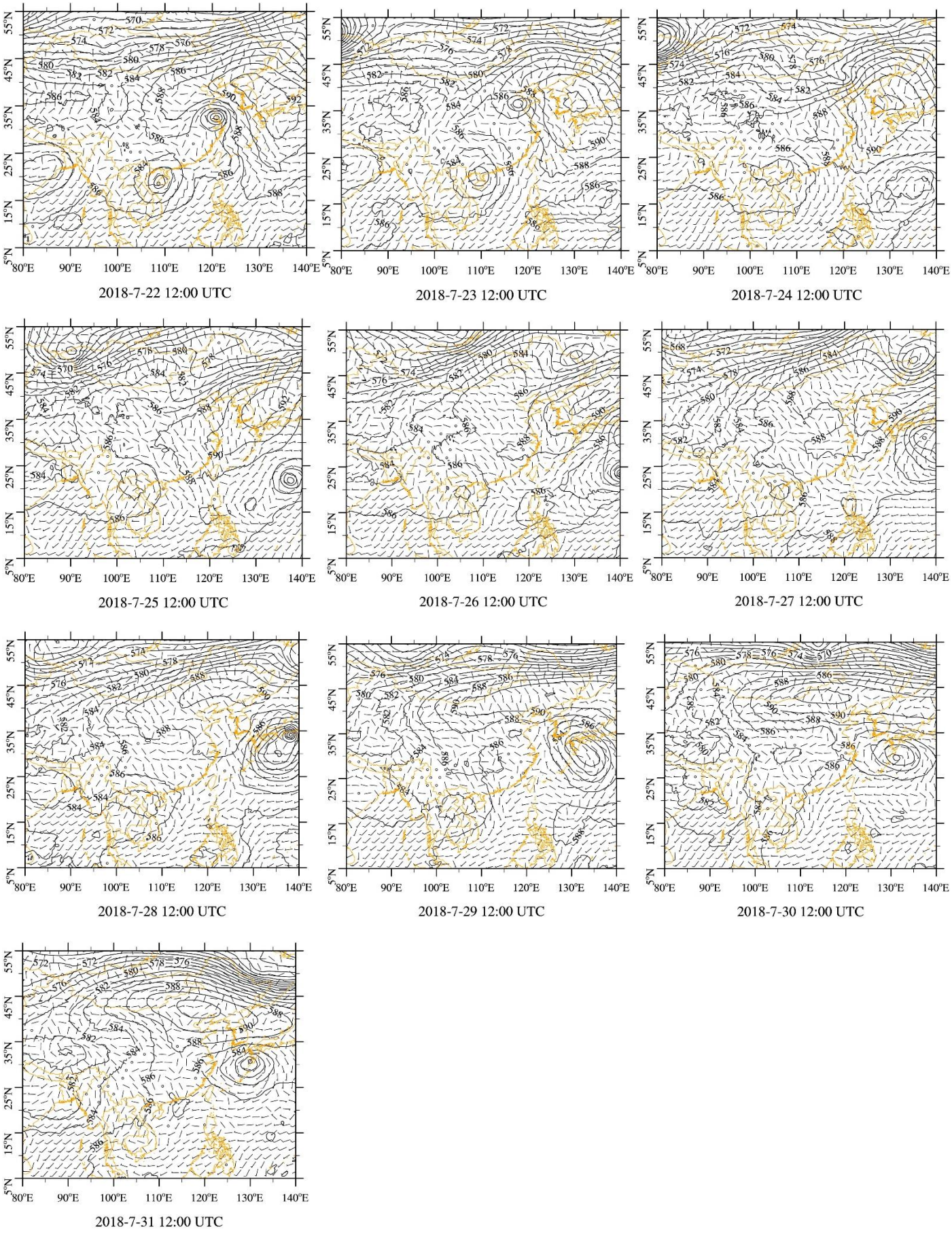

Figure S4. Synoptic situation at 500hPa from 10th to 31th July.

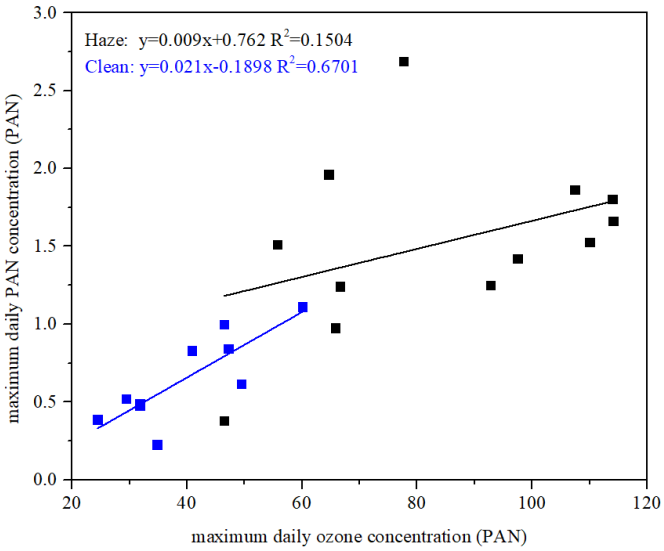

Figure S5. Correlation between PAN and O_3 daily maximum concentrations during haze and clean.

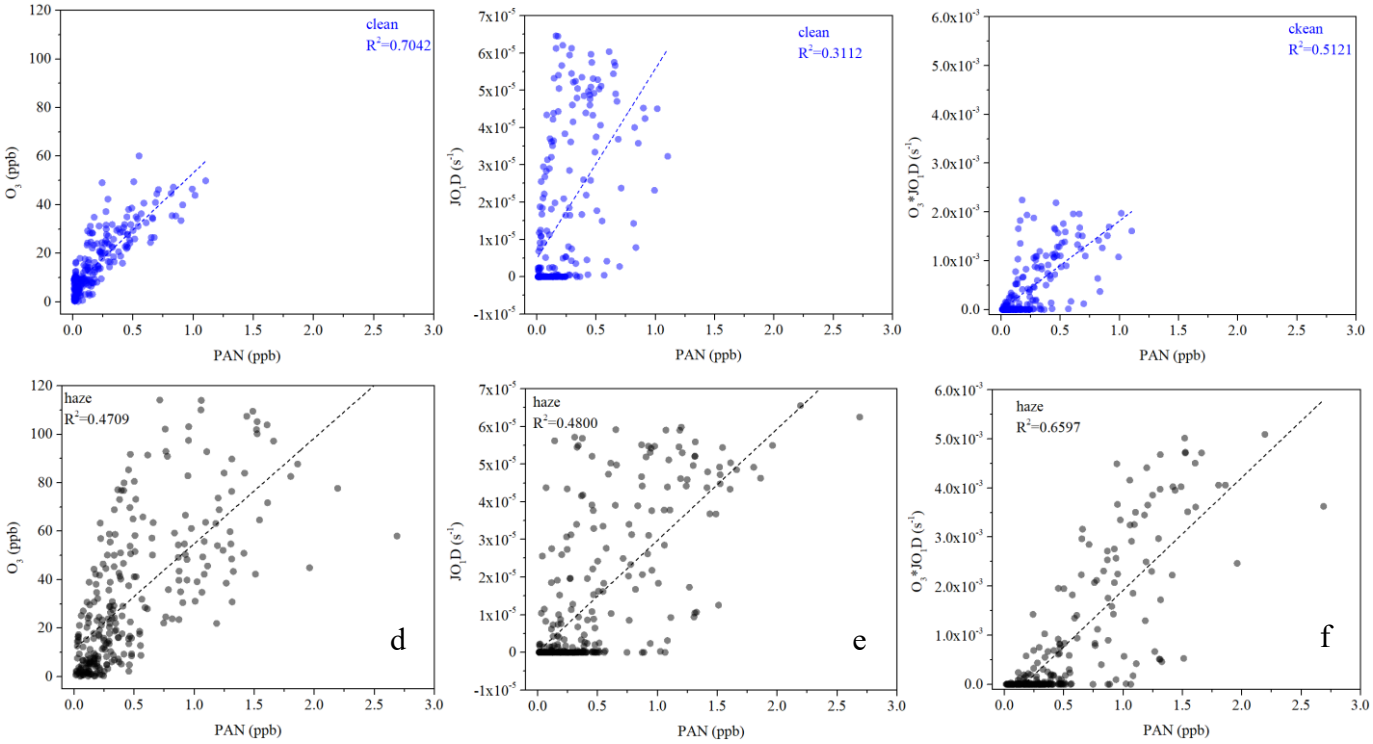

Figure S6. a, b, and c are scatter plots of PAN with O_3, JO_1D, and their product during the cleaning period, while d, e, and f are scatter plots of PAN with O_3, JO_1D, and their product during the haze period. The darker the color, the denser the data points.

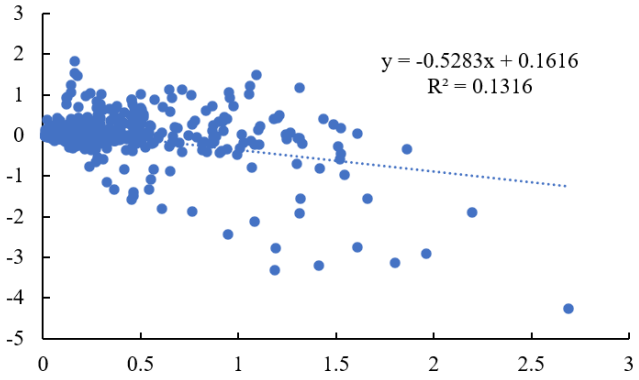

Figure S7. Scatterplot of PAN concentration observed and net rates of PAN simulated during 10-31 July 2018.

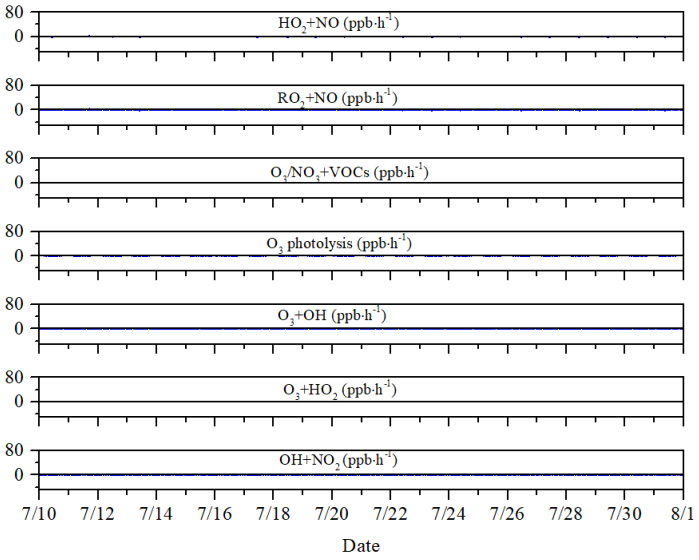

Figure S8. Time series plot of the reaction of HO_2+NO, RO_2+NO, O_3/NO_3+VOCs, O_3 photolysis, O_3+OH, O_3+HO_2, and OH+NO_2.

Reference

Ghahremanloo, M., Lops, Y., Choi, Y., and Yeganeh, B.: Deep Learning Estimation of Daily Ground-Level NO_2 Concentrations From Remote Sensing Data, J. Geophy. Res.: Atmos., 126, 10.1029/2021jd034925, 2021.

Hodson, T. O.: Root-mean-square error (RMSE) or mean absolute error (MAE): when to use them or not, Geosci. Model Dev., 15, 5481-5487, 10.5194/gmd-15-5481-2022, 2022.

Liu, T., Chen, G., Chen, J., Xu, L., Li, M., Hong, Y., Chen, Y., Ji, X., Yang, C., Chen, Y., Huang, W., Huang, Q., and Wang, H.: Seasonal characteristics of atmospheric peroxyacetyl nitrate (PAN) in a coastal city of Southeast China: Explanatory factors and photochemical effects, Atmos. Chem. Phys., 22, 4339-4353, 10.5194/acp-22-4339-2022, 2022.

Xu, W., Zhang, G., Wang, Y., Tong, S., Zhang, W., Ma, Z., Lin, W., Kuang, Y., Yin, L., and Xu, X.: Aerosol Promotes Peroxyacetyl Nitrate Formation During Winter in the North China Plain, Environ. Sci. Technol., 55, 3568-3581, 10.1021/acs.est.0c08157, 2021.

Xue, L., Wang, T., Wang, X., Blake, D. R., Gao, J., Nie, W., Gao, R., Gao, X., Xu, Z., Ding, A., Huang, Y., Lee, S., Chen, Y., Wang, S., Chai, F., Zhang, Q., and Wang, W.: On the use of an explicit chemical mechanism to dissect peroxy acetyl nitrate formation, Environ. Pollut., 195, 39-47, 10.1016/j.envpol.2014.08.005, 2014.

Zeng, L., Fan, G. J., Lyu, X., Guo, H., Wang, J. L., and Yao, D.: Atmospheric fate of peroxyacetyl nitrate in suburban Hong Kong and its impact on local ozone pollution, Environ. Pollut., 252, 1910-1919, 10.1016/j.envpol.2019.06.004, 2019.